# 行政院國家科學委員會專題研究計畫　期中進度報告

## 金屬奈米線模型之研究(中法國合計畫)(1/2)

計畫類別：個別型計畫
計畫編號：NSC93-2113-M-002-018-
執行期間：93 年 02 月 01 日至 94 年 01 月 31 日
執行單位：國立臺灣大學化學系暨研究所

計畫主持人：彭旭明
共同主持人：王瑜，李豐穎，蘇明德

報告類型：精簡報告
報告附件：國際合作計畫研究心得報告
處理方式：本計畫可公開查詢

中　華　民　國 93 年 11 月 30 日

Annual Report of Modelling Metal Nanowires

The metal string complexes with different metal ions and various lengths have been synthesized and structurally characterized recently by Prof. Peng in National Taiwan University. Their potential served as molecular metalwire and logic switch in future nanomachinery applications attracts great attention. In light of these important future applications, a joint effort between Taiwan and France with theoreticians and experimentalists is devoted to characterize the bonding and structures of these metal string complexes and their oxidized products. The physical and chemical properties of these complexes with various transition metals are calculated by employing ab initio method, such as Gaussian98 and DFT. This report is divided into two parts. One is to study the conductivity of these complexes by performing the band structure calculation. The other one is to simplify ligand to study the magnetic properties.

Part I. Ligand simplification of linear metal nanowires

In this study, we would like study magnetic properties of the metal nanowire from $[Ni_3(\mu_3\text{-dpa})_4Cl_2]$ (dpa = *syn-syn* bis(a-ptridyl)amino) to $[Ni_5(\mu_5\text{-tpda})_4Cl_2]$ (tpda = tripyridyldiamino) and $[Ni_7(\mu_7\text{-teptra})_4Cl_2]$ (teptra = tetrapyridyltriamino), and they can be denoted as $Ni_nL_4Cl_2$ or $Ni_n$ for n=3, 5 and 7. Figure 1 shows the values of magnetic susceptibility of of Ni3, Ni5 and Ni7 complexes, which are believed to be strongly dependent on the Ni-Ni distances. The calculation demand of these metal nanowires is beyond the current computational capacity available in Taiwan, especially when the size of the metal nanowires increases. In order to reduce the calculation loading, we simplify the ligand component by replacing dpa with several similar ligands and manipulating the final structure of metal wire, such as distance of Ni-Ni and Ni-Cl bond. Through this effort, we hope to investigate the spin distribution of metal ions along the metal nanowires. There are six different kinds of ligands which have been tested, such as $HN(CH)N)_2H$, $CH_3N((CH)N)_2CH_3$, $HN_5H$, $CH_3N_5CH_3$, $HN((CCl)N))_2H$, and $HN((CBr)N)_2H$ and their corresponding structures are shown in Figure 2. Note that $HN_5H$ has been adapted by Prof. F. A. Cotton (*Inorg. Chem.* **1998**, *37*, 4066) to simplify the hpp ligand. The results of $Ni_3L_4Cl_2$ with above six ligands were summarized in Table 1. In the Table 1, the $\Delta E$ represents the energy difference, in kcal/mol, between the high spin and low spin of $Ni_3L_4Cl_2$. Judged from the Ni-Ni distances of those optimized structures, we found the $HN((CCl)N)_2H$ ligand is a proper candidate among these ligand, but the characteristics of the $HN((CCl)N)_2H$ ligand are somewhat different from dpa. Even though the distance of Ni-Ni of this simplified ligand are a little longer than that of the original ligand, we still take the $HN((CH)N)_2H$ as the substituted model of dpa since the trend of magnetic properties for Ni3, Ni5 and Ni7 complexes is main concern in

this study.

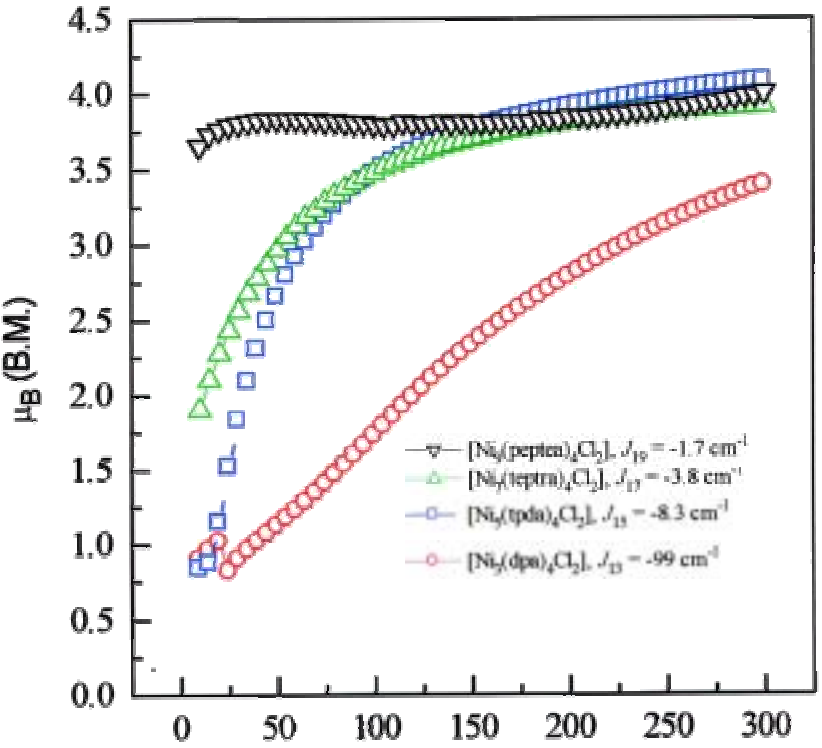


Figure 1 The antiferromagnetic coupling constant for $Ni_n$ for n=3, 5, 7 and 9

Table 1: (U)B3LYP/LanL2DZ calculated results.

| Ligand | $HN_5H$ | | $CH_3N_5CH_3$ | | $HN((CBr)N)_2H$ | | $HN((CCl)N)_2H$ | |
|---|---|---|---|---|---|---|---|---|
| | High spin | Low spin | High spin | Low spin | High spin | Low spin | High spin | Low spin |
| Symmetry | D4h | D4h | D4h | D4h | D4h | D4h | D4h | D4h |
| **Diatances** | | | | | | | | |
| Ni-Ni | 2.506 | 2.613 | 2.517 | 2.446 | 2.436 | 2.451 | 2.449 | 2.469 |
| Ni-Cl | 2.326 | 2.352 | 2.402 | 2.598 | 2.385 | 2.528 | 2.382 | 2.519 |
| $Ni_{term}$-N | 2.078 | 2.085 | 2.114 | 1.998 | 1.975 | 1.895 | 1.978 | 1.899 |
| $Ni_{center}$-N | 1.955 | 1.948 | 1.943 | 1.891 | 2.196 | 2.069 | 2.169 | 2.044 |
| $<S^2>$ | 6.043 | | 6.096 | | 6.172 | | 6.156 | |
| $\Delta E^a$ | 0 | 141.50 | 0 | -11.15 | 0 | 19.20 | 0 | 16.70 |

Table1-Continue: (U)B3LYP/LanL2DZ calculated results.

| Ligand | dpa[b] | | dpa[c] | | $HN((CH)N)_2H$ | | $CH_3N((CH)N)_2CH_3$ | |
|---|---|---|---|---|---|---|---|---|
| | High spin | Low spin | High spin | Low spin | High spin | Low spin | High spin | Low spin |
| Symmetry | D4 | D4 | D4 | D4 | D4h | D4h | D4h | D4h |
| **Diatances** | | | | | | | | |
| Ni-Ni | 2.457 | 2.381 | 2.490 | 2.406 | 2.646 | 2.504 | 2.661 | 2.540 |
| Ni-Cl | 2.453 | 3.04 | 2.418 | 2.976 | 2.368 | 2.571 | 2.398 | 2.736 |
| $Ni_{term}$-N | 2.102 | 1.954 | 2.112 | 1.962 | 2.068 | 1.931 | 2.111 | 1.979 |
| $Ni_{center}$-N | 1.914 | 1.910 | 1.921 | 1.914 | 1.944 | 1.931 | 1.924 | 1.901 |
| $<S^2>$ | 6.013 | | 6.013 | | 6.013 | | 6.012 | |
| ΔE | | 23.17 | 0 | 28.41 | 0 | 22.43 | 0 | 27.26 |

[a]ΔE represents the energy difference, in kcal/mol, between the high spin and low spin of $Ni_3L_4Cl_2$. [b]Data from results of P. Kiehl, M.-M. Rohmer and M. Benard. [c]In this work.

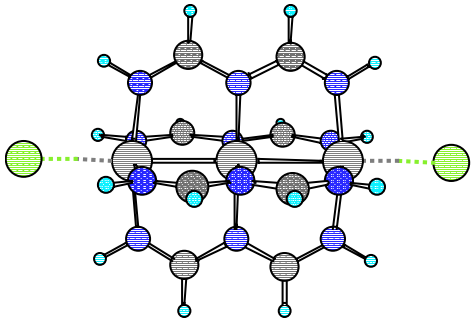

$Ni_3(H(CH)N)_2H)_4Cl_2$

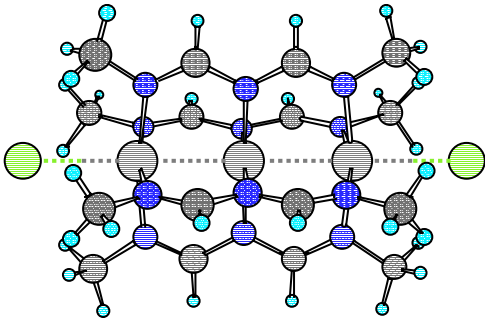

$Ni_3(CH_3(CH)N)_2CH_3)_4Cl_2$

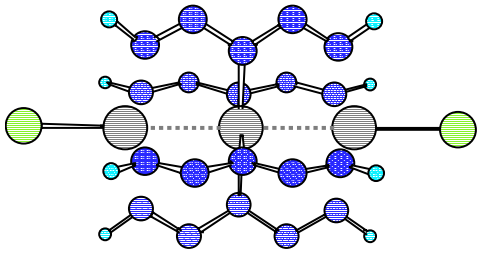

$Ni_3(HN_5H)_4Cl_2$

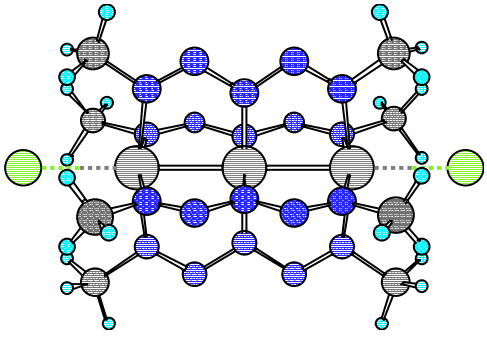

$Ni_3(CH_3N_5CH_3)_4Cl_2$

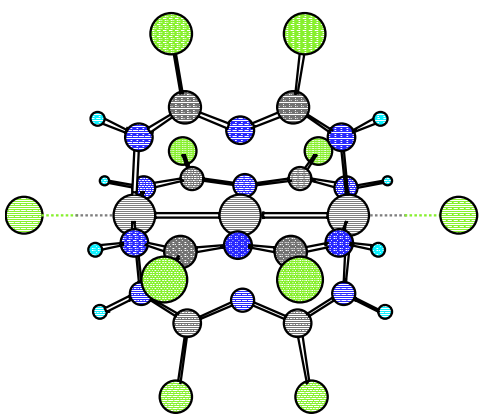

$Ni_3(H(CClN)_2H)_4Cl_2$

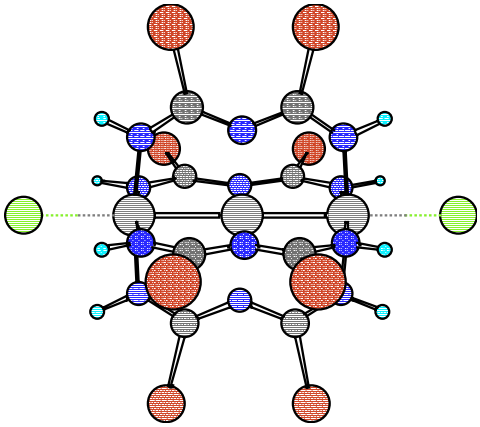

$Ni_3(CH_3(CBrN)_2CH_3)_4Cl_2$

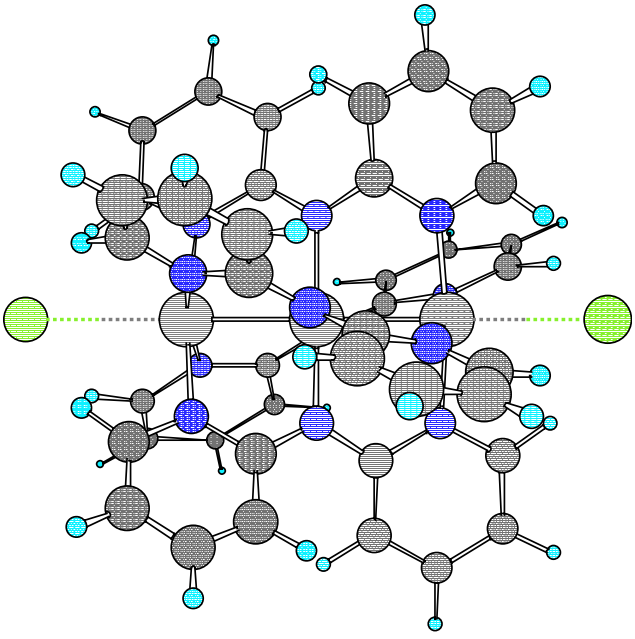

$Ni_3(dpa)_4Cl_2$

Figure 2. The structures of the original and six simplified ligands.

We performed the structures optimization using B3LYP/LanL2DZ method. Table 2 list the spin density and found the properties of $HN((CH)N)_2H$ as ligands is similar the original ligand, *i.e.*, dpa.

Table 2: The Mulliken spin density of Ni3 complexes in high spin

| Ligand | dpa[a] | dpa[b] | HN((CH)N)$_2$H |
|---|---|---|---|
| Symmetry | D4 | D4 | D4h |
| **Diatances** | | | |
| $Ni_{term}$ | +1.59 | +1.63 | +1.64 |
| $Ni_{center}$ | +0.11 | +0.06 | 0.06 |
| Cl | +0.09 | +0.10 | +0.13 |
| $Ni_{term}$ | +0.07 | +0.06 | +0.06 |
| $Ni_{center}$ | +0.01 | +0.01 | -0.00 |
| $<S^2>$ | 6.013 | 6.013 | 6.013 |

[a] Data from results of P. Kiehl, M.-M. Rohmer and M. Benard. [b] In this work

In following study, we present the optimized results using B3LYP/LanL2MB method. The start points are those structures found previous with B3LYP/LanL2DZ to find the structure of $Ni_5$ and $Ni_7$ complexes using higher level DFT method, because the energy of $Ni_3$ cluster with high spin is higher than with low spin and it is opposite to the result using B3LYP/LanL2DZ method. In Scheme 1, we present the experimental data of Ni-Ni and Ni-N distances of tri-, penta-, and hepta- nonanickel(II) $[Ni_3(\mu_3\text{-dpa})_4Cl_2]$ , $[Ni_5(\mu_5\text{-tpda})_4Cl_2]$ and $[Ni_7(\mu_7\text{-teptra})_4Cl_2]$ complexes. The dpa, tpda and eptra are the *syn-syn* bis(α-ptridyl)amino, tripyridyldiamino and tetrapyridyltriamino, respectively.

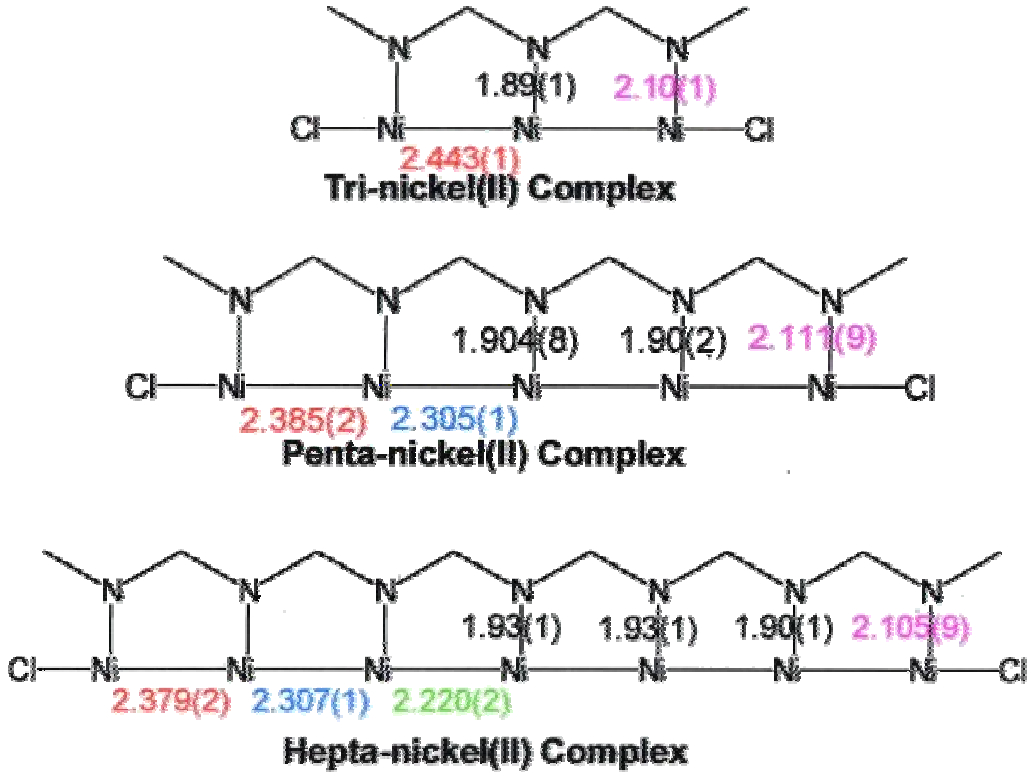


Scheme 1

The results indicate that the distance of Ni-Ni bond decreases and the distance of Ni-N bond increases as the size of metal nanowires increases. The distance of terminal Ni-Ni and Ni-N bonds always are longer than the others. Except the terminal Ni-N bond, the distance of central Ni-N bonds always is longer than the others. The shortest Ni-Ni bond locates at the central position. Our calculated $Ni_3$ complex structure with $HN((CH)N)_2H$ in high spin using B3LYP/LanL2MB is shown in Figure 3

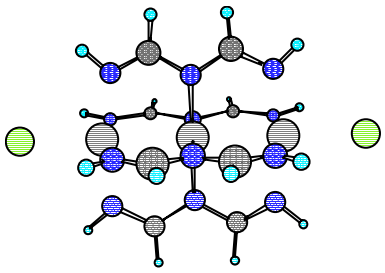

Figure 3. The optimal structure of $Ni_3$ with the simplified ligand in high spin.

The distance of Ni-Ni, Ni-Cl, Ni-Nterm and Ni-Ncenter are 2.635, 2.409, 2.045 and 1.914 A, respectively. It close to the result of using B3LYP/LanL2DZ optimized method. The corresponding $Ni_5$ complex is shown in Figure 4.

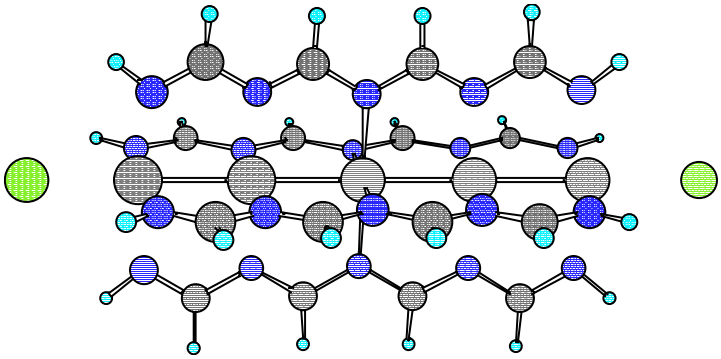

Figure 3. The optimal structure of $Ni_5$ with the simplified ligand in high spin.

The distance of terminal Ni-Ni and center Ni-Ni are 2.487 and 2.465 A. It shows that the central Ni-Ni bond is shorter than the terminal Ni-Ni bond and is consistent with the results of the x-ray structure. The distances of Ni-N from left to central part are 2.064, 2.016 and 1.965, respectively. It showed the terminal Ni-N bond is the longest one in the entire Ni-N bond and it is also consistent with the results of the x-ray structure. The corresponding $Ni_7$ complex is shown in Figure 4

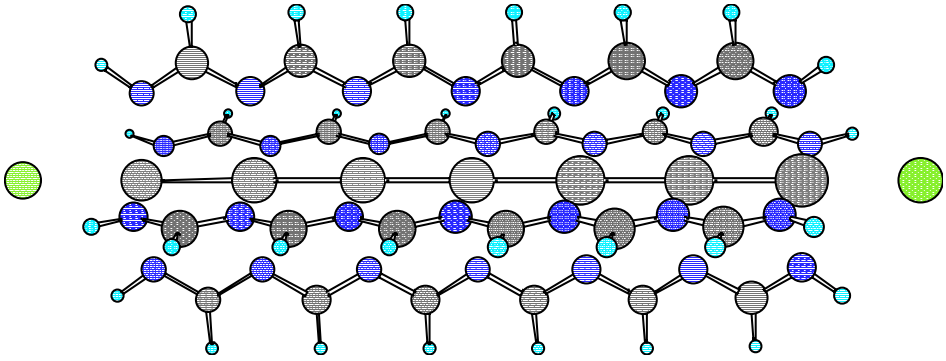

Figure 3. The optimal structure of $Ni_7$ with the simplified ligand in high spin.

The distance of Ni-Ni bond from left to right are 2.473, 2.392 and 2.374, respectively. The distance of Ni-Ni bond from left to right is 2.473, 2.392 and 2.374, respectively. The distance of Ni-N bond from left to right is 2.047, 2.049, 2.064 and 2.073,

respectively. In conclusion, we found that with simplified ligand, such as $HN((CH)N)_2H$, the trend of the Ni-Ni and Ni-N distances, which depends on the number of Ni, is consistent with the observation found in experimental results.

Part II. Electronic properties of linear metal nanowires

The abilities to produce, manipulate and to study nanometer scale structures developed immensely over year have opened up the possibilities for the design and construction of molecular-scale equivalents of solid-state devices.[1-3] Among those nanostructures, the metallic lines connecting active devices on a chip have been recognized to play a decisive role in determining the functionality and reliability of future integrated circuit industry.[1] Single-wall nanotubes have been considered to be ideal conducting nanowires due to their high yields[4], structural uniformity and metallic properties of particular varieties of the highly symmetric structures[5]. Still much effort has been devoted to construct metallic connection in molecular scale. With the rapidly advanced fabrication technology, metallic nanowires have been created by mechanically breaking a fine metal wire [6], by separating a tip and a flat substrate [7-9], or two macroscopic electrodes in contact [10], by anodizing Al nanowires with an atomic force microscope [11], and by electrochemical deposition [12,13]. All the methods mentioned above have difficulties in maintaining the uniformity in both detail atomic scale size and structure of the nanowires. We calculate the electronic properties of organometallic complexes $[M_n(\mu_n\text{-peptea})_4Cl_2]$, where M is an metal ion and n is the number of the metal ions, has been successfully synthesized and crystallized for various numbers of metal ions with a defined length by several research groups (see Fig. 1).[14-17] We refer this particular type of linear organometallic complexes as LOM complexes from now on.

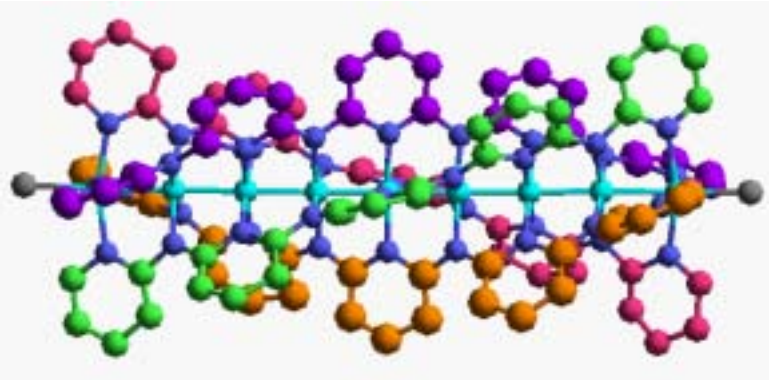

**Figure 1.** Crystal structure of $[Ni_9(\mu_9\text{-(peptea)}_4Cl_2)(C_2H_4Cl_2)_{10}$ [15]. Ligands are drawn in different colors to show the helix structure around the metal chain (in azure).

There are several properties of the LOM complexes worth close attentions. Firstly, the structure of the LOM complexes maintains almost the same regardless the kinds and number of metal ions. [14] Secondly, the metal-metal distance also remains almost the same no matter the kinds or number of metal ions. [16]. Thirdly, the

organic ligands of the LOM complexes surround the central metal ions in a form of helix structures, which increases the overall structural stability. [14] Finally, the length and structure of the LOM complexes can be controlled precisely through experimental means; and the length of the LOM is steadily increasing, for example the number of the metal ions in Ni LOM complex has been increasing from 3, 4, 5, 7 up to 9[16,18]. With above advantages, the LOM complexes can be served as potential metallic connections between nanodevices provided that the central metal ions possess metallic behavior with high conductivity. The purpose of this study is to examine the electronic properties of the LOM complexes through band structure calculation.

With the steady increase in size of the LOM complexes, theoretical works on this type of organometallic complexes have mainly used gas-phase clusters at semi-empirical level. Here we propose to use periodic boundary conditions to study the electronic properties of a hypothetic infinite one-dimensional metalwires from the first principle to examine the possibility of using the LOM complexes as conducting nanowires. In the light of $D_4$ symmetry of the LOM complexes, the molecular models, which we used in calculations, were constructed from the crystal structure of the $[Ni_9(\mu_9\text{-peptea})_4Cl_2]$ [15], with $[M_4(\mu_4\text{-dpda})_4]_n$ as the repeat unit, where M can be Ni, Cr, Co metal ions and dpda is dipyridyldiamido moiety. We refer these hypothetic infinite LOM complexes as HILOM nanowires. The direction of the HILOM nanowires is set along z axis. The *ab initio* quantum mechanical calculations were performed with academic and commercial (MSI) versions of CASTEP 3.9 code. [19,20] Gradient-corrected density functional theory [21,22] (DFT) is used to calculate the electronic ground-state of the system expanding the valence electronic wavefunctions in plane-waves up to a 290 eV cut-off and representing the nuclei and core electrons by ultrasoft pseudopotentials. The structures of these HILOM nanowires are first optimized with BFGS technique and then calculate the band structure. For the band structure calculations, we sampled 11 K-points along the nanowire direction. Due to the possibilities of metallic behavior for these nanawires, we added 4 more extra bands than the number of filled bands as in the insulator case.

The results of the band structure calculations and corresponding density of states for the Ni, Cr, Co HILOM nanowires are shown in Fig. 2 and 3. The fermi levels are -1.39, -2.63 and -2.09 eV for the Ni, Co and Cr HILOM nanowires respectively. We noticed that the general patterns between the band structures of the Ni and Co HILOM nanowires are very similar. By further examining the corresponding density of states of these HILOM nanowires, we found that actually the overall pattern among the

density of states for these three different nanowires share the same pattern. There is a wide energy band gap between -1.0 and -2.5 eV for the Ni HILOM nanowire and a gap between -0.75 and -2.6 eV for the Co HILOM nanowire at the origin of the Brillouin zone, but both of the gaps gradually reduces to zero at the boundary of the Brillouin zone. It is why that there is a region with very small population roughly between -1.39 and -2.63 eV in both of Ni and Co HILOM nanowires, and the small hump in this region indicates the location where two energy bands meet (see Fig. 2). Interestingly, -1.39 and -2.63 eV are the fermi levels for the Ni and Co HILOM nanowires respectively. Due to this observation, the Ni and Co HILOM nanowires might be semi-metallic because even though there is no band gap around the fermi level, the density of states between valence band and conduction band is so low that it should possess some properties of insulator. As to the Cr HILOM nanowire, there is substantial density of states between valence band and conduction band, which might indicate that it is a metallic. In order to the possible conducting mechanisms, we investigate the HOMO and LUMO bands of these HILOM nanowires. The HOMO band of the Ni HILOM nanowire at fermi level consists of anti-bonding interactions between Ni $d_z^2$ orbitals and between Ni($d_{xy}$)-N($p$) orbitals. The LUMO orbital is formed by the anti-bonding interactions between Ni($d_{xy}$)-Ni($d_{x^2-y^2}$) orbitals and between Ni($d_{xy}$)-N($p$) orbitals. The HOMO and LUMO bands of the Co HILOM nanowire are similar to those found in Ni HILOM nanowire. Considering the small ionization potential and the shallow conduction band of this complex, its conduction behavior under electron donor/acceptor doping would be interesting. The HOMO orbital of the Cr HILOM nanowire is rather delocalized and mainly constituted by $d_{xy}$ and $d_{x^2-y^2}$ orbitals of chromium and p ortibals of carbon in the teptra ligands. The LUMO is localized on the chromium chain, and composed by $d_{z^2}$ of chromium orbital.

We have presented a first-principle electronic band-structure calculation on three different HILOM nanowires. Our preliminary results indicate that the Ni, Co, and Cr HILOM nanowires are metallic since there are no band gaps around the fermi level. Especially, Cr HILOM nanowire might possess metallic behavior and can serve as conducting wire in future nanomachinery applications. The Co and Ni HILOM nanowires are semi-metal since the limited available states around the fermi levels.

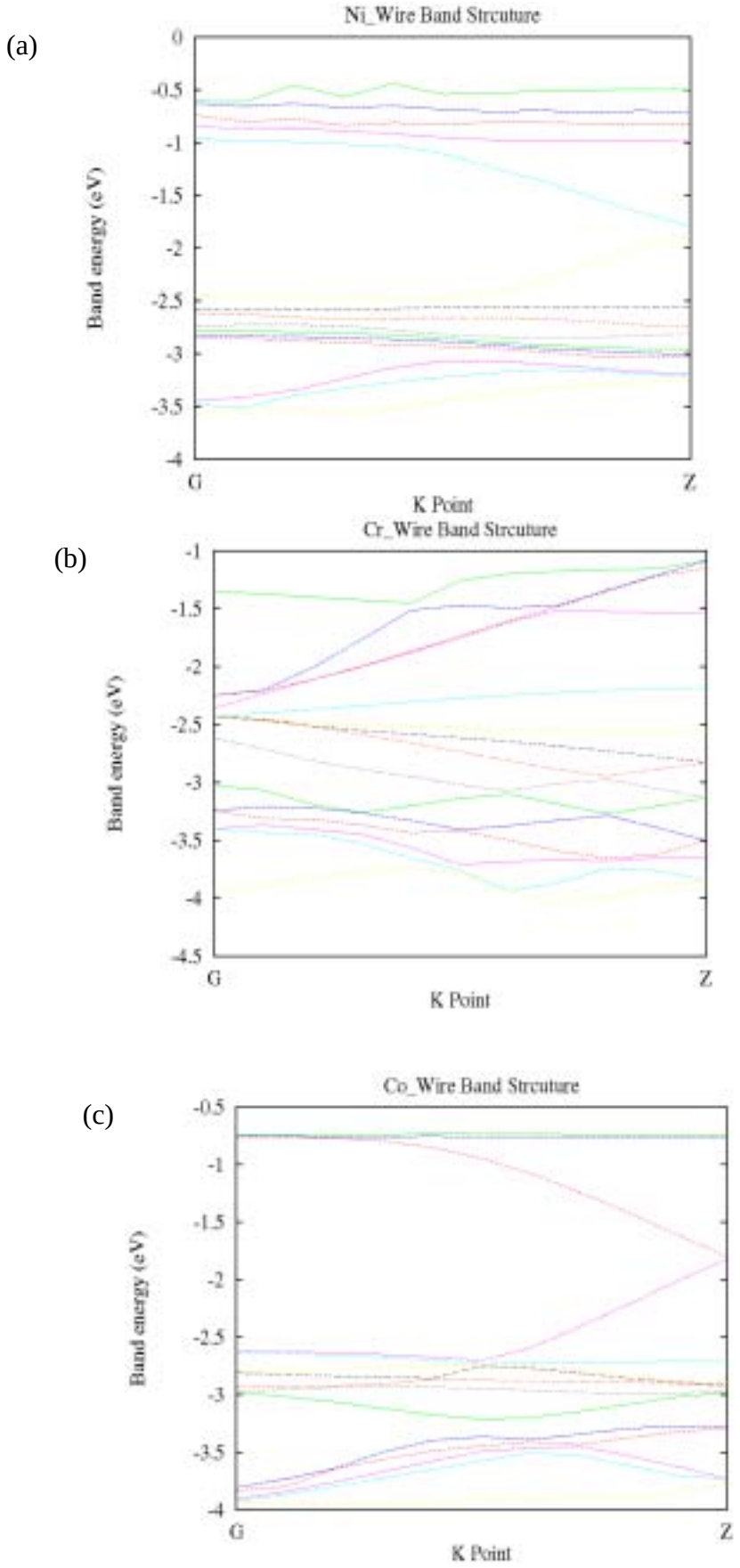


Figure 2. The band-structure of HILOM nanowires. (a), (b) and (c) are band-structure

of Ni, Cr, and Co HILOM nanowires accordingly. Ten of the highest-energy occupied bands are plotted along with four of lowest-energy unoccupied bands.

(a)

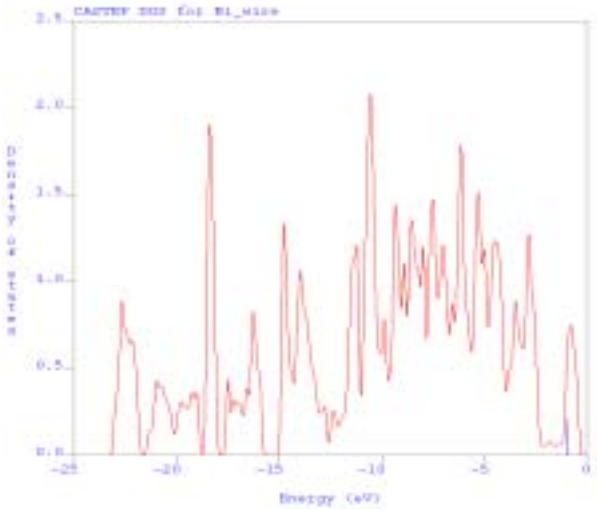

(b)

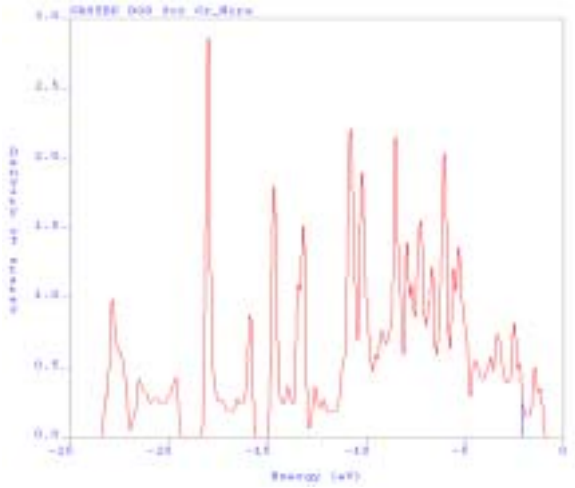

(c)

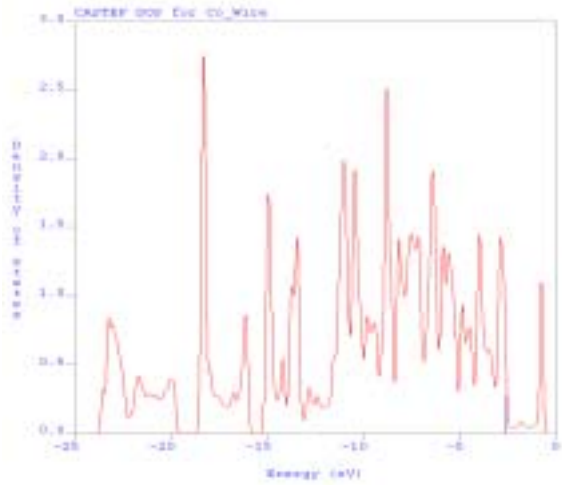

Figure 3. The density of state for HILOM nanowires. (a), (b) and (c) are density of state for Ni, Cr, and Co HILOM nanowires accordingly. The blue bars inside the plots are the fermi levels.

**Reference**


1. A. N. Korotkov, in *Molecular Electronics*, edited by J. Jortner and M. Ratner (Blackwell Science, Oxford, 1997).
2. D. L. Klein, R. Roth, A. K. L. Lim, A. P. Alivisatos, and P. L. McEuen, *Nature* **389**, 699 (1997).
3. D. Goldhaber-Gordon, H. Shtrikman, D. Mahalu, D. Abusch-Magder, U. Meirav, and M. A. Kastner, *Nature* **391**, 156 (1998).
4. S. Iijima and T. Ichhashi, *Nature* **363**, 603 (1993).
5. N. Hamada, S.-I. Sawada and A. Oshiyama, *Phys. Rev. Lett.* **68**, 1579 (1992).
6. J. M. Krans, J. M. van Ruitenbeek, V. V. Fisun, I. K. Yanson, and L. J. de Jongh, *Nature* **375**, 767 (1995).
7. J. I. Pascual, J. Mendez, J. Gomez-Herrero, A. M. Baro, N. Garcia, U. landman, W. D. Leuedtke, E. N. Bogachek, and H.-P. Cheng, *Science* **267**, 1793 (1995).
8. G. Rubio, N. Agrait, and S. Vieeira, *Phys. Rev. Lett.* **76**, 2302 (1996).
9. L. Oleson, E. Lagsgaard, I. Stensgaad, F. Besenbacher, J. Schiotz, P. Stoltze, K. W. Jacobsen, and J. K. Norskov, *Phys. Rev. Lett.* **72**, 2251 (1994).
10. J. L. Costa-Kramer, N. Garcia, P. Garcia-Mochales, and P. A. Serena, *Surf. Sci.* **342**, L1144 (1995).
11. E. S. Snow, D. Park, and P. M. Campbell, *Appl. Phys. Lett.* **69**, 269 (1996).
12. C. Z. Li and N. J. Tao, *Appl. Phys. Lett.* **72**, 894 (1998).
13. E. Braun, Y. Eichen, U. Sivan and G. Ben-Yoseph, *Nature* **391**, 775 (1998).
14. S. J. Shieh, C. C. Chou, G. H. Lee, C. C. Wang, and S. M. Peng, *Angew. Chem. Int. Ed. Engl.* **36**, 56 (1997).
15. Y. H. Chen, C. C. Lee, C. C. Wang, G. H. Lee, S. Y. Lai, F. Y. Li, C. Y. Mou and S. M. Peng, *Chem. Commun.* 1667 (1999).
16. C. C. Wang, W. C. Lo. C. C. Chou, G. H. Lee, J. M. Chen and S. M. Peng, *Inorg. Chem.* **37**, 4059 (1998).
17. F. A. Cotton, L. M. Daniels, C. A. Murillo and X. Wang, J. Chem. Soc. Dalton Trans. 517 (1999).
18. S.-M. Peng, C.-C. Wang, Y.-L. Jang, Y.-H. Chen, F.-Y. Li, C.-Y. Mou, M.-K. Leung, Journal of Magnetism and Magnetic Materials, 80, 2000.
19. M. C. Payne, M. P. Teter, D. C. Allan, T. A. Arias, T. A. Johnnopoulos, J. Johnnopoulos, *Rev. Mod. Phys.* **64**, 1045 (1992).
20. Cerius$^2$ User Guide, Molecular Simulations, San Diego, CA, 1997.
21. P. Hohenberg, W. Kohn, *Phys. Rev.* **136**, B864 (1964).
22. W. Kohn, L. J. Sham, *Phys. Rev.* **140**, A1133 (1965).